Tree Physiology 00, 1–15
https://doi.org/10.1093/treephys/tpac148

Research paper

Zearalenone regulates microRNA156 to affect the root development of *Tetrastigma hemsleyanum*

Jiangshan Li[1], Xiaoping Huang[1], Zhanghui Zeng[1], Zhehao Chen[1], Jinxin Huang[1], Chenjing He[1] and Taihe Xiang[1,2,3]

[1]College of Life and Environmental Sciences, Hangzhou Normal University, Hangzhou 311121, China; [2]Zhejiang Provincial Key Laboratory for Genetic Improvement and Quality Control of Medicinal Plants, Hangzhou 311121, China; [3]Corresponding author (xthcn@163.com); (xthcn@hznu.edu.cn)

Received July 16, 2022; accepted December 21, 2022; handling Editor Nathaniel Street

Zearalenone (ZEN) is a secondary metabolite from *Fusarium* species. It is also present in plants and regulates the photochemical reaction in Photosystem II, the stress response and root growth. To investigate the mechanism by which ZEN regulates *Tetrastigma hemsleyanum* root growth, differentially expressed microRNAs (miRNAs) were identified and verified by high-throughput sequencing and *Agrobacterium rhizogenes*-mediated transformation of the roots of *T. hemsleyanum* seedlings treated with and without ZEN. The predicted functions of microRNA156b (miR156b) and microRNA156f (miR156f) were confirmed in transgenic hairy roots. (i) A total of 70 miRNAs showed significantly different expression levels under ZEN treatment, including seven highly conserved miRNAs. (ii) The number of lateral roots and total root length of the transgenic hairy roots overexpressing miR156b and miR156f was significantly higher than the wild-type hairy roots, and thus the overexpression of miR156b and miR156f in *T. hemsleyanum* promoted lateral root development. (iii) Bioinformatics analysis predicted that the target genes of miR156b and miR156f were *SPL9*/*10*. As compared with the wild-type hairy roots, the expression of *SPL9* was significantly lower in the hairy roots overexpressing miR156b, and the expression of *SPL10* was significantly lower in the hairy roots overexpressing miR156f. Therefore, *SPL9* could be the target gene of miR156b, and *SPL10* could be the target gene of miR156f. This study shows that ZEN could increase the expression of miR156b and miR156f in *T. hemsleyanum* roots, which negatively regulated the expression of their putative target genes *SPL9* and *SPL10*, consequently promoting the growth and development of the lateral roots.

Keywords: microRNA156, root, *Tetrastigma hemsleyanum* Diels & Gilg ex Diels, zearalenone.

Introduction

Zearalenone (ZEN), also known as F-2 toxin, was first isolated from maize with *Fusarium* head blight. It is a secondary metabolite mainly produced by *Fusarium* species, including *F. graminearum*, *F. tricinctum*, *F. culmorum*, *F. equiseti*, *F. semitectum* and *F. solani* (Ma et al. 2013; Munkvold 2017), and it predominantly contaminates maize, wheat, rice, barley, millet and oat. In animals, ZEN acts as an estrogen that leads to abnormal reproductive function, acute and chronic poisoning, and even death, causing huge economic losses to livestock farms (Gautier et al. 2020; Rai et al. 2020).

ZEN has also been found in plants. Li et al. (1980) first detected ZEN in the wheat stem apex, and its fluctuations were highly synchronized with vernalization in winter wheat during the overwintering period. It has been reported in *Zea mays*, *Apium graveolens*, *Triticum aestivum*, *Sorghum bicolor*, *Glycine max*, *Gossypium hirsutum*, *Beta vulgaris* and microalgae and has been found to influence plant growth and development (Li et al. 1980; Meng et al. 1989; Li and Meng 1989; Bosch and Mirocha 1992; Fu and Meng 1994; Mally et al. 2016; Filek et al. 2019; Eagles et al. 2019). Yao et al. (1991) showed that ZEN promoted callus formation in *Nicotiana tabacum*. Using *N. tabacum*, *Daucus carota* subsp. *sativus*, *Cucumis sativus*

and *Brassica napus*, Yao and Meng (1991) found that a low concentration of ZEN promoted callus formation and growth, a high concentration of ZEN inhibited callus formation and growth, whereas an appropriate concentration of ZEN enhanced embryoid formation and vegetative growth, but delayed flowering. Moreover, the concentration-dependent effects of ZEN vary among plants. Zhao and Meng (1999) found that exogenous ZEN could enhance the cold resistance of winter wheat, affect the content of abscisic acid and promote wheat growth during the jointing stage. Biesaga-Kościelniak et al. (2003) reported that ZEN could stimulate the growth of haploid wheat embryos. Kościelniak et al. (2011) reported that the incubation of seeds in a ZEN solution resulted in an increase in the photochemical efficiency of Photosystem (PS) II in soybean seedlings but did not induce any response in PSII in wheat at medium illumination. When added to NaCl solutions during the germination period, ZEN contributed to reducing the growth inhibition of wheat seedlings. Weigt et al. (2019) reported that a significant increase in microspore embryogenesis effectiveness on media with the addition of ZEN was observed both at the stages of its induction and the formation of green plants in some genotypes of wheat. Furthermore, ZEN also improved the induction of microspore embryogenesis.

On the other hand, microRNAs (miRNAs) belong to a subset of endogenous hairpin-derived small RNAs that post-transcriptionally control target gene expression, and mostly transcription factors. Plant miRNAs have been shown to be master regulators of development and stress responses in plants (Couzigou and Combier 2016; Barrera-Rojas et al. 2021). Among the various plant miRNAs with diverse functions, miR156 plays a key role in biological processes (Jerome Jeyakumar et al. 2020).

The tuberous root of the plant *Tetrastigma hemsleyanum* is used as a traditional Chinese medicine (Xiang et al. 2021). Previously, an endophytic fungal strain TH15 was isolated from the roots of *T. hemsleyanum* and was identified as belonging to *Fusarium* (Huang et al. 2022). The metabolites of TH15 promoted the root growth of *T. hemsleyanum* (Song et al. 2017). Further investigation indicated that ZEN was a metabolite of TH15 based on enzyme-linked immunosorbent assay, and ZEN addition promoted the growth of *T. hemsleyanum* seedlings (Wang et al. 2022). However, the molecular mechanism by which ZEN regulates *T. hemsleyanum* root development remains unclear. In this study, high-throughput miRNA sequencing and functional validation in transgenic hairy roots were performed to investigate the regulatory mechanism of ZEN on *T. hemsleyanum* root development at the molecular level.

Materials and methods

Materials

The plantlets of *T. hemsleyanum* came from our previous study (Du et al. 2015). Plantlets at the same growth stage were selected and cultured in 1/2 Murashige & Skoog (MS) solid medium supplemented with 0.1 mg/L ZEN (treatment) and 1/2 MS solid medium (control) for 15 days (Wang et al. 2022). The culture was incubated at 22 ± 2 °C with a 12-h photoperiod of 1,500–2,000 lux light level. Then, all roots were cut from the plants and collected for experimentation.

Extraction of RNA and construction of miRNA sequencing library

The RNA was extracted using a Total RNA Purification kit (Cat. TRK1001, LC Sciences, USA), and miRNA sequencing library was constructed using a TruSeq Small RNA Sample Prep kit (Illumina, San Diego, USA). The extraction and construction were performed according to the kit instructions. The quality of the total RNA was assessed separately using 1% agarose gel electrophoresis and a NanoPhotometer spectrophotometer (IMPLEN, CA). The RNA samples with a 260/280 ratio of 1.8–2.0, a 260/230 ratio of 2.0–2.5 and an RNA integrity number of >8.0 were used for sequencing. The miRNA sequencing libraries were constructed from 1 μg of qualified total RNA in each sample, and a Bioanalyzer 2,100 (Agilent, CA, USA) was used to evaluate the quality of the library.

Sequencing of miRNA and bioinformatics analysis

Single-end sequencing was performed on a HiSeq 2,500 sequencer (Illumina, San Diego, USA) with a read length of 1 × 50 bp. Clean reads (18–25 nt) were obtained by removing raw reads with adaptors, which were aligned to sequences in several RNA databases and effectively filtered to obtain valid reads. The miRNA data were analyzed using ACGT101-miR (LC Sciences, Houston, TX, USA). Valid reads were aligned to the precursor and mature miRNA sequences of reference species in the miRBase 22.0 database. The precursor sequences were aligned to the *T. hemsleyanum* transcriptome sequences (GenBank accession: GIXF00000000) to identify known and novel miRNAs.

The miRNA expression profiling was performed using normalized data (Li et al. 2016). The secondary structures of mature miRNAs with matched precursor sequences were drawn using the online software RNA Folding Form V2.3 (http://www.unafold.org). The precursor sequences of mature miRNAs without matched precursor sequences were obtained by extension (120 bp) of the matched mature miRNA sequences in the genomes and then visualized. A heatmap of differential miRNAs was plotted showing the mean normalized read number using OmicStudio tools (http://www.omicstudio.cn). Pearson's distance measurement and complete linkage were used for clustering.

Annotation of predicted target genes was performed by alignment of the miRNA sequences using the NCBI BLAST tool against the non-redundant (nr) (Yang et al. 2006), Swiss-Prot

(Wu et al. 2006), Gene Ontology (GO) (Ashburner et al. 2000) and Kyoto Encyclopedia of Genes and Genomes (KEGG) (Kanehisa and Goto 2000) databases. The GO functional enrichment analysis of the target genes was performed using the ClusterProfiler package (Yu et al. 2012). The degree of KEGG pathway enrichment was represented by an enrichment factor, and the *P*-values indicating the significance of the enrichment were calculated using Fisher's method.

Validation of sequencing data

For validation of the sequencing data, nine known miRNAs and one predicted miRNA were randomly selected to conduct fluorescence quantitative PCR (qPCR) using the poly(A) tailing method (Balcells et al. 2011), and U6 snRNA was selected as the reference gene based on the report by Luo et al. (2018). The first strand of cDNA of miRNA was synthesized using the miRNA first strand cDNA synthesis kit (Accurate Biology, Hunan, China). Ligation of poly(A) tail to miRNA and reverse transcription were performed at 37 °C for 60 min. The obtained cDNA was diluted 10 times with RNase-free water and stored at −20 °C for the next step. Additionally, the SYBR Green Premium Pro Taq HS qPCR kit (Accurate Biology, Hunan, China) was used to analyze miRNA expression. The reaction conditions were 50 ng/μL of cDNA template, 1 μmol/L of each primer, 10 μL of 2× SYBR Green Pro Taq HS Premix and 6.4 μL RNase-free water in a final volume of 20 μL. The PCR procedure underwent initial denaturation at 95 °C for 30 s followed by 40 cycles of 95 °C for 5 s and 60 °C for 20 s. The melt curve was acquired at 60–95 °C. The primer sequences are shown in Table S1 available as Supplementary data at *Tree Physiology* Online.

Bioinformatics analysis of miR156 and construction of miR156b and miR156f overexpression vectors

The sequences of pre-miR156b and pre-miR156f in *Vitis vinifera* (grape) were aligned against the transcript sequences of *T. hemsleyanum* in NCBI to obtain miR156b and miR156f precursors. The secondary structures of the predicted pre-miR156b and pre-miR156f were determined using the online software RNA Folding Form V2.3. Primers were designed with Primer Premier 6 by targeting the untranslated regions of the two transcripts (Table S2 available as Supplementary data at *Tree Physiology* Online), and the amplification products included a 444-bp fragment containing MIR156b and a 133-bp fragment containing MIR156f. The amplified DNA fragments were ligated into the pESI-T vector (Yeasen, Shanghai, China) and sequenced. The DNA fragments were also ligated into pRI101-AN-gfp (Du et al. 2015) to construct the plant expression vectors pRI101-AN-gfp-miR156b and pRI101-AN-gfp-miR156f containing a green fluorescent protein gene.

Induction of transgenic hairy roots of T. hemsleyanum and characterization by molecular and fluorescence techniques

The recombinant vectors were transformed into *Agrobacterium rhizogenes* K599 using the freeze–thaw method. According to the method of Du et al. (2015), the transformed K599 was used to infect the leaves of *T. hemsleyanum* seedlings to obtain transgenic hairy roots. The hairy roots were cultured in B5 medium with cefotaxime and then sub-cultured four times to completely remove *A. rhizogenes*. Bacteria-free hairy roots were propagated in B5 medium, and the hairy root DNA was extracted using a Plant Genomic DNA Extraction kit (Tiangen Biotech, China). Primers were designed based on the sequences of *rolC* (Tong et al. 2018) in the T-DNA of *A. rhizogenes* K599 and *gfp* sequence (GenBank accession number: U17997). The primers were synthesized by Sangon Biotech (Shanghai, China), and the primer sequences are shown in Table S3 available as Supplementary data at *Tree Physiology* Online. Transgenic hairy roots were observed under a confocal laser-scanning microscope (LSM710, ZEISS, Germany) using blue laser excitation and an FITC filter.

Phenotype of the transgenic hairy roots and expression of miR156 and target genes

Root tips (~1 cm in length) were cut from transgenic and wild-type (WT) hairy roots and cultured in B5 medium at 25 °C in the dark for 30 days. Twenty roots were collected from each group for analysis of lateral root number, total root length and root diameter using a root phenotyping system (TOP Cloud-agri Technology, Zhejiang, China). Meanwhile, the hairy roots of the WT plant, plant overexpressing miR156b (miR156b OE) and plant overexpressing miR156f (miR156f OE) were cultured for 30 days and used for total RNA extraction with a Spin Column Plant Total RNA Purification kit (Sangon, Shanghai, China). The expression of miR156 was determined using the SYBR Green Premium Pro Taq HS qPCR kit (Accurate Biology, Hunan, China), according to the above-mentioned method. The predicted target genes were detected by quantitative reverse-transcription (qRT)-PCR according to the method described by Xiang et al. (2021). The reaction system was configured according to the instructions of the One Step RT-qPCR kit (BBI Life Sciences, USA). The reaction was run on the fluorescence qPCR instrument (CFX96) (Bio/Rad Co. Ltd, USA). The *GAPDH* gene was selected as an internal reference gene (Yuan et al. 2020), and three technical replicates were used for each reaction. The PCR procedure underwent pre-denaturation at 95 °C for 2 min, followed by 40 cycles of 95 °C for 10 s, 55 °C for 31 s and 72 °C for 30 s. The melting curve was determined at 65–95 °C. The absorbance value was determined every 0.5 °C/5 s. The $2^{-\Delta\Delta Ct}$ method was used to calculate the relative expression of the target gene (Pfaffl 2001). Three independent experiments were performed. The primer sequences are shown

in Table S4 available as Supplementary data at *Tree Physiology* Online.

Statistical analysis

The data were analyzed using SPSS20.0 software (IBM Corp., Armonk, NY, USA), and statistical significance was determined by Student's *t*-test.

Results

High-throughput miRNA sequencing

A total of 86,838,333 raw reads were generated from the miRNA sequencing of triplicate samples with and without ZEN treatment (Table S5 available as Supplementary data at *Tree Physiology* Online). The raw reads were processed, aligned against the mRNA, Rfam and Repbase databases and filtered to obtain valid reads (Table S6 available as Supplementary data at *Tree Physiology* Online). The length distribution of the valid reads showed that 24-nt miRNAs were most abundant (Figure S1 available as Supplementary data at *Tree Physiology* Online), which is in line with typical miRNAs and indicates high sequencing accuracy. Pearson's correlation analysis revealed a high correlation ($\geq$0.98) between the biological replicates (Figure S2 available as Supplementary data at *Tree Physiology* Online). The miRNAs were classified into five groups. From these, reads were compared with the precursors of the known reference species in the miRBase database, and the precursors were further compared with the genome, which was called gp1b (Table S7 available as Supplementary data at *Tree Physiology* Online). There was no whole-genome data of *T. hemsleyanum*, so we focused on the gp1b group to identify miRNA. From the gp1b group, 56 known miRNAs belonging to 20 miRNA families were identified (Table S8 available as Supplementary data at *Tree Physiology* Online). The known miRNA families were miR156, miR159, miR319, miR160, miR162, miR164, miR166, miR167, miR168, miR169, miR171, miR319, miR393, miR394, miR396, miR477, miR535, miR858, miR2916 and miR5141. The miRNA expression was classified into low, middle and high levels based on the normalized expression data. Most of the miRNAs with high expression were members of conservative miRNA families such as miR156, miR166, miR167 and miR396. The remaining valid reads were aligned to the *T. hemsleyanum* de novo transcriptome using miRDeep 2 software (Friedländer et al. 2008; Williamson et al. 2013). Based on the formation of hairpin structures that met the 11 criteria in the miRDeep 2 software by the sequences obtained by extension from the genomic matches, a total of 232 novel miRNAs were identified (Table S9 available as Supplementary data at *Tree Physiology* Online). We analyzed the first base preference of the novel miRNAs and found a preference of 'A' for 18, 20 and 23–25 nt and a preference towards 'U' for 19 nt and 21–22 nt (Figure S3 available as Supplementary data at *Tree Physiology* Online).

Differential expression of miRNAs

The root expression of 70 miRNAs differed significantly under ZEN treatment relative to the control (Table S10 available as Supplementary data at *Tree Physiology* Online and Figure 1). Among the differential miRNAs, 29 were from 12 known miRNA families (e.g., miR156, miR396 and miR168), and 41 were novel miRNAs. Of the known miRNAs, 21 were upregulated and eight were downregulated. Of the novel miRNAs, 26 were upregulated and 15 were downregulated. There were six members of the miR156 family: miR156b, miR156c, miR156e, miR156f, miR156g and miR156h. The expression of miR156b and miR156f was significantly upregulated in the roots treated with ZEN, whereas the other three members did not show significant differences.

V. vinifera is closely related to *T. hemsleyanum,* and both species belong to the Vitaceae family. Thus, the known miRNAs of *V. vinifera* were used as a reference to identify seven highly conserved miRNAs with 100% identity and known functions (Table 1). Of these miRNAs, five were upregulated and two were downregulated. Notably, the expression of miR156b and miR156f was significantly upregulated in the roots treated with ZEN. To assess the reliability of the miRNA sequencing results, 10 miRNAs were selected from known and novel miRNAs (vvi-miR482, vvi-miR482_L + 1, vvi-miR3623-5p, vvi-miR403a, vvi-miR156b, vvi-miR156f, mtr-miR172c-5p, ath-miR858b, mes-miR535a and PC-3p-6025_918). The relative expression levels of vvi-miR482, vvi-miR482_L + 1, vvi-miR3623-5p, vvi-miR403a, vvi-miR156b, vvi-miR156f, mes-miR535a and PC-3p-6025_918 were upregulated in the treatment groups compared with the control groups as measured by qRT-PCR, which was consistent with the results of high-throughput sequencing. In addition, the relative expression levels of mtr-miR172c-5p and ath-miR858b were downregulated in the ZEN treatment groups compared with the control groups as measured by qRT-PCR, which was also consistent with the high-throughput sequencing results. (Figure 2). qRT-PCR analysis further indicated that the sequencing data were reliable.

Prediction and enrichment analysis of differential miRNA target genes

The GO functional annotation was performed on the target genes of miRNAs that were differentially expressed in *T. hemsleyanum* roots with and without ZEN treatment (Figure 3). The GO enrichment showed that the target genes were significantly enriched in 20 GO terms such as regulation of transcription, response to strigolactone, regulation of meristem growth and plant organ development (Figure 4). The KEGG pathway enrichment showed that the target genes were enriched in

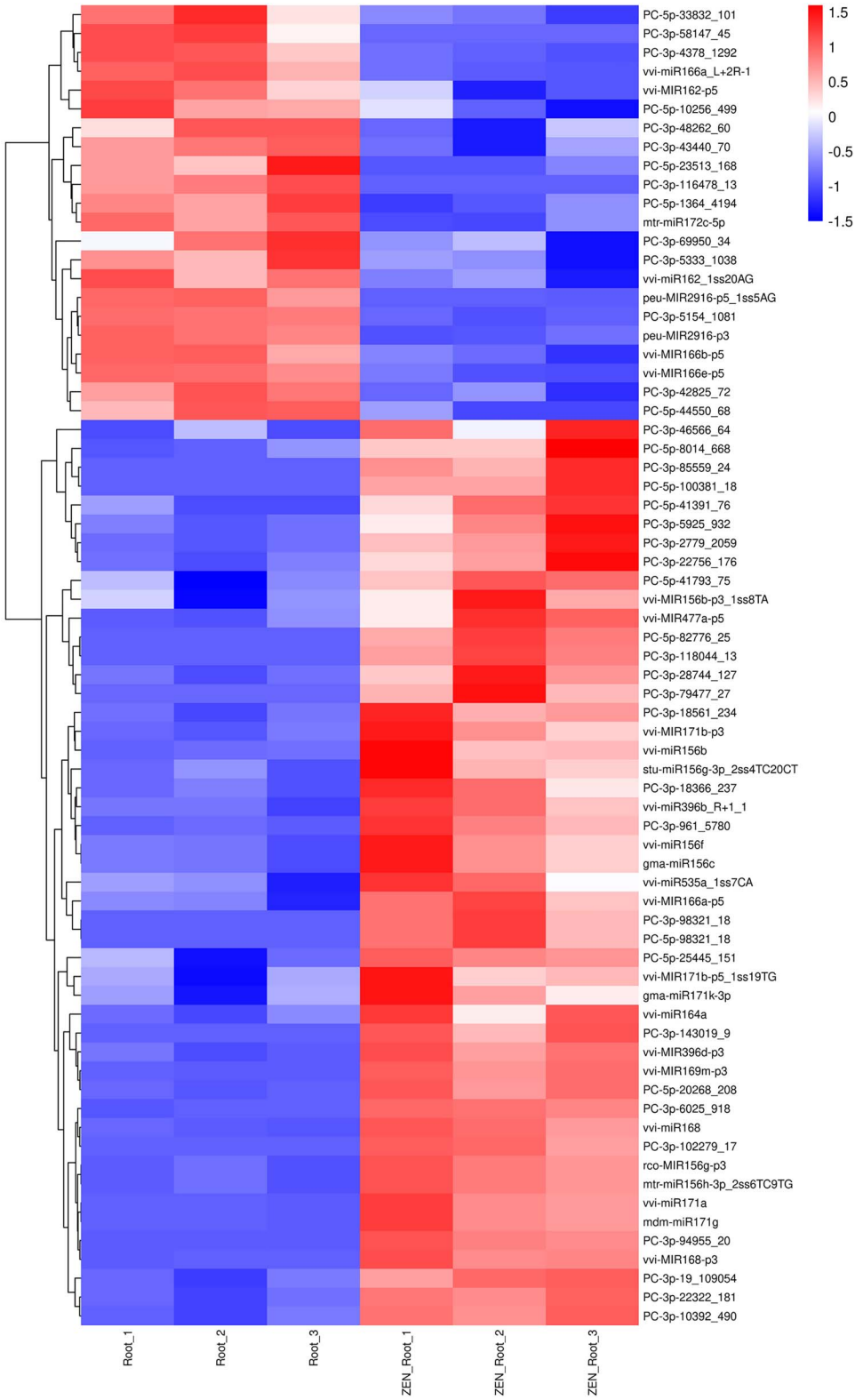

Figure 1. Heatmap of differentially expressed miRNA.

20 pathways such as starch and sucrose metabolism, plant–pathogen interaction, plant-hormone signal transduction and NOD-like receptor signaling pathway (Figure 5).

Secondary structures of the miR156 precursors

According to previous studies (Gao et al. 2018; Barrera-Rojas et al. 2020; Yun et al. 2022), the expression of

Table 1. Differentially expressed and highly conservative miRNAs and their candidate target genes.

Name of miRNA perfectly matched grapes	Sequence	Expression of treated with ZEN *vs* non-treated with ZEN	Function of target gene
vvi-miR156b	TGACAGAAGAGAGTGAGCAC	up	Squamosa promoter-binding-like protein 9/10
vvi-miR156f	TTGACAGAAGATAGAGAGCAC	up	Squamosa promoter-binding-like protein 9/10
vvi-MIR166a-p5	AATGAGGTTTGATCCAAGATC	up	MAPKKK, YODA
vvi-miR171a	TGATTGAGCCGTGCCAATATC	up	GRAS family transcription factor
vvi-miR164a	TGGAGAAGCAGGGCACGTGCA	up	NAC domain transcription factor
vvi-MIR166b	GGAATGTTGGCTGGCTCGAGG	down	transcription factor PIF4
vvi-MIR166e-p5	GGAATGTTGTCTGGCTCGAGG	down	RNA polymerase Rpb7 protein

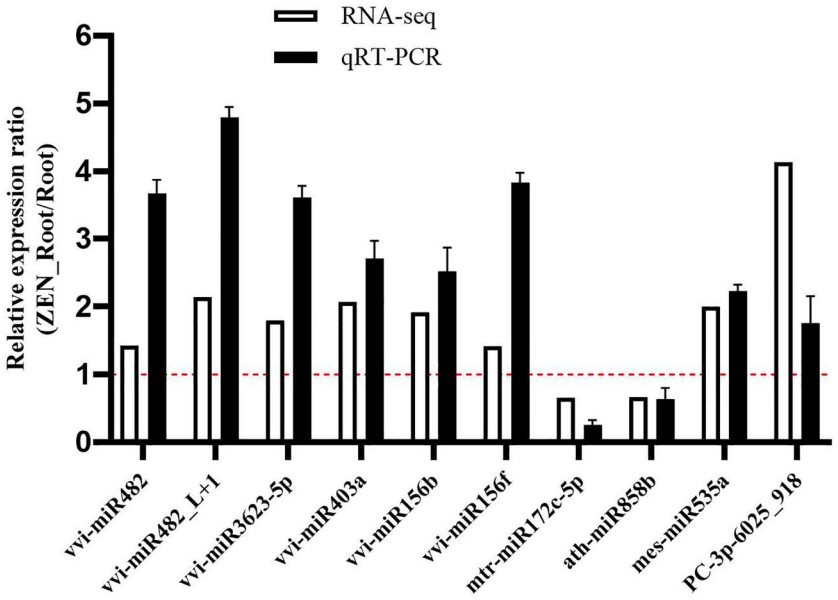

Figure 2. Confirmation of the miRNA sequencing results by qRT-PCR. The amount in the ordinate shows the relative expression ratio of the ZEN treatment group relative to the control group.

miRNA156 is closely related to root development. Therefore, miRNA156b and miR156f, which were differentially expressed, were selected for further analysis. The secondary structures of pre-miR156b and pre-miR156f were predicted by bioinformatics analysis, and the minimum folding free energy was −45.20 and −44.80 kcal/mol, respectively (Figure S4 available as Supplementary data at *Tree Physiology* Online).

Construction of miRNA156 overexpression vectors and induction of transgenic hairy roots

The recombinant vectors pRI101-AN-gfp-miR156b and pRI101-AN-gfp-miR156f were verified by restriction endonuclease digestion (Figure S5 available as Supplementary data at *Tree Physiology* Online) and sequencing (data not shown). Transgenic hairy roots were obtained by infecting the leaves of *T. hemsleyanum* seedlings with *A. rhizogenes* K599 carrying the recombinant plasmids (Figure 6).

Five hairy roots overexpressing miR156b or miR156f were randomly selected for PCR amplification with *rolC* and *gfp* primers to generate a 433-bp band and a 497-bp band, as expected (Figure 7). In addition, transgenic hairy roots overexpressing miR156b or miR156f emitted intense green fluorescence under excitation by blue light, whereas the hairy roots induced by the WT K599 did not show fluorescence under excitation (Figure S6 available as Supplementary data at *Tree Physiology* Online).

Phenotypic analysis of the transgenic hairy roots

After 1 month of cultivation, the transgenic hairy roots overexpressing miR156b or miR156f showed significant differences in morphology as compared with the WT hairy roots (Figure 8). The numbers of lateral roots of miR156b OE and miR156f OE were about one and four times, respectively, higher than that of the WT. Both transgenic hairy root lines showed more branches but similar root diameters relative to the WT line (Table 2).

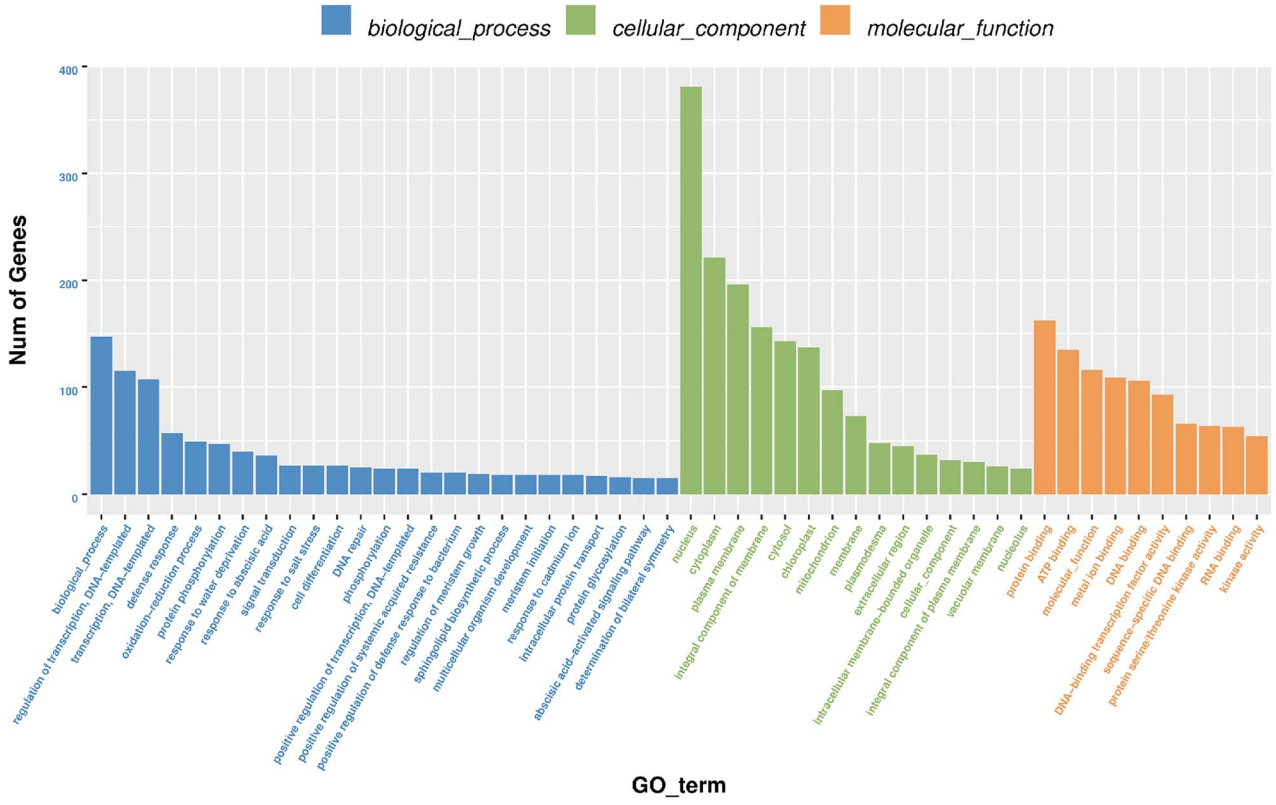

Figure 3. Annotation of the GO function of the target gene of the differentially expressed miRNAs.

Table 2. Phenotypic analysis of transgenic hairy roots.

Name of hairy root	Number of lateral roots	Root length (mm)	Average root diameter (mm)
WT	14.67 ± 4.50c	155.14 ± 39.56b	2.70 ± 0.04a
miR156b OE	28.67 ± 2.87b	600.81 ± 23.93a	2.77 ± 0.07a
miR156f OE	69.67 ± 4.49a	704.28 ± 2.19a	2.73 ± 0.05a

Note: WT: wild type hairy root; miR156b OE: miR156b-overexpressing hairy root; miR156f OE: miR156f-overexpressing hairy root; the different lowercase letters in a column indicate significant differences ($P < 0.05$)

qRT-PCR analysis of miR156 and target gene expression in the transgenic hairy roots

Compared with the WT line, the expression of miR156b and miR156f in the corresponding transgenic lines was significantly upregulated by 1.73-fold and 3.21-fold, respectively. The relative expression of *SPL9* was significantly downregulated in miR156b OE but not significantly different in miR156f OE, whereas the relative expression of *SPL10* was significantly downregulated in miR156f OE but not affected in miR156b OE (Figure 9).

Discussion

miRNAs play an important regulatory role in the growth and development of plant roots. Bao et al. (2014) found that the overexpression of miR396a in *Arabidopsis thaliana* reduced the transcription of its target genes *GRF* and *bHLH74* and resulted in shorter roots. The overexpression of miR775 in *A. thaliana* significantly increased the length of the primary roots by inhibiting the expression of its target gene encoding galactosyl transferase (Gaddam et al. 2021), whereas the overexpression of miR167a in *Populus* inhibited the transcription of its target gene and promoted lateral root development (Cai et al. 2019). Using high-throughput sequencing, Tang et al. (2020) identified 145 miRNAs associated with the development of sweet potato storage roots. Zhou et al. (2020) reported that miRNAs and their target genes could regulate the nitrate uptake rate in the different root zones of poplar.

Of particular interest is the function of miR156. In *A. thaliana*, the overexpression of miR156 resulted in the production of more lateral roots, and the miR156 target genes *SPL3*, *SPL9* and *SPL10* were involved in the suppression of lateral root growth. Specifically, miR156/*SPL* regulated lateral root growth by activating the expression of *AGL79*, and *SPL10* played a

Figure 4. GO enrichment analysis of the target genes for differentially expressed miRNAs.

predominant role (Yu et al. 2015; Gao et al. 2018; Barrera-Rojas et al. 2020). Furthermore, miR156 modulated phase change through its temporal expression in the shoot, and the miR156-regulated *SPL* genes repressed adventitious root development (Xie et al. 2012; Xu et al. 2016). The *MIR156* and *SPL* genes had opposing expression patterns during primary root growth (Zhang et al. 2020). In *Malus xiaojinensis*, the high expression of miR156 was necessary for auxin-induced adventitious root formation via *MxSPL26*, but was independent of *MxPINs* and *MxARFs* expression in leafy cuttings (Xu et al. 2017). In alfalfa (*Medicago sativa*), transgenic plants overexpressing miR156 and with *SPL13* silenced showed an increased number of lateral branches, delayed flowering and elevated biomass production (Aung et al. 2015). Moreover, miRNA156 could improve the drought tolerance of *M. sativa* by silencing the expression of *SPL13* (Arshad et al. 2017). It has been reported that miR156

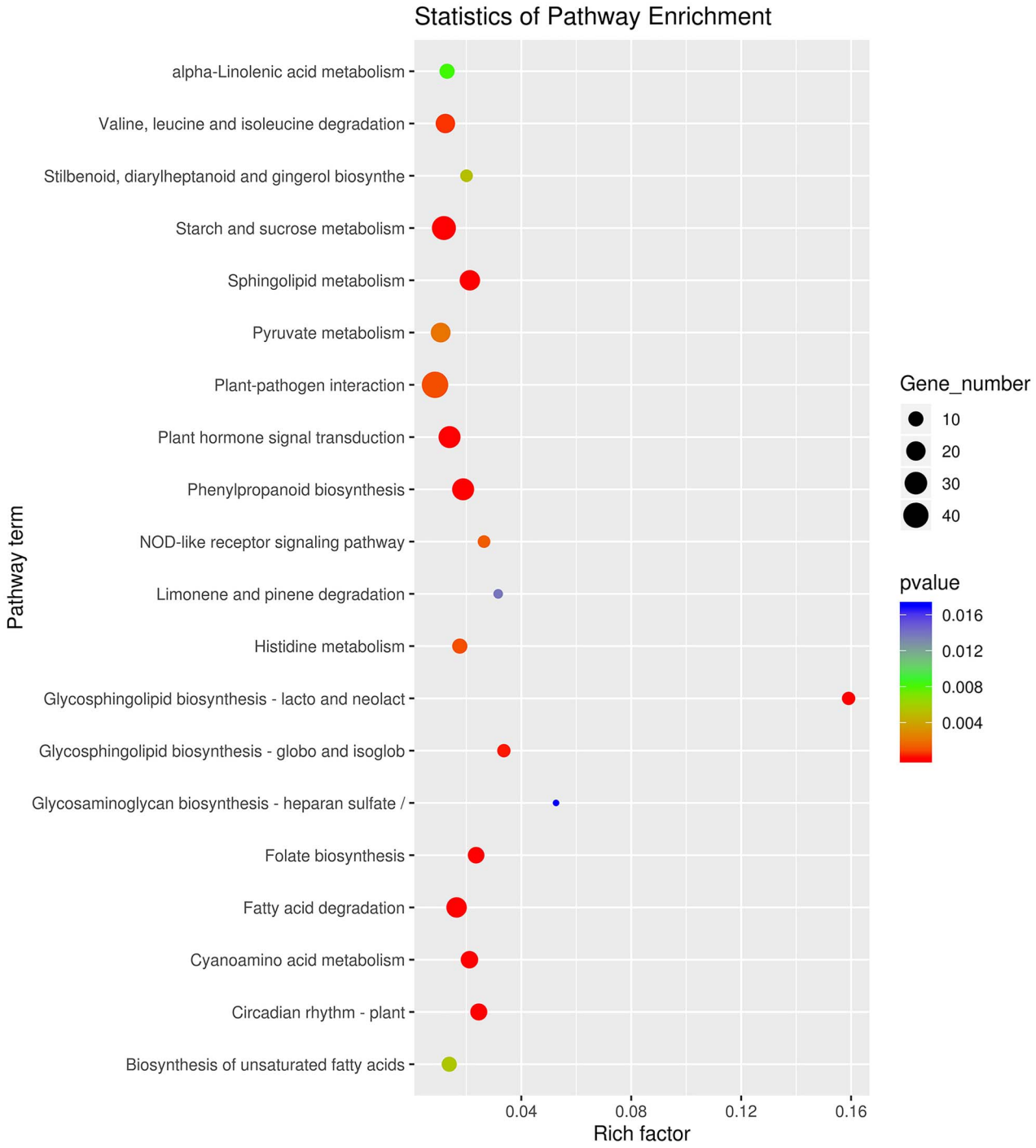

Figure 5. KEGG pathway enrichment analysis of the target genes for differentially expressed miRNAs.

plays a regulatory role in root regeneration and phytohormone biosynthesis (Aung et al. 2017). In soybean (*G. max*), the overexpression of miR156b significantly increased the number of long branches as well as the number of pods and seeds, and therefore the yield of each plant (Sun et al. 2019).

In the present study, the roots of seedlings treated with and without ZEN were used to identify the differentially expressed miRNAs by high-throughput sequencing, and their target genes and gene functions were analyzed. The expression of miR156b and miR156f was significantly upregulated in the roots treated with ZEN (Table 1 and Figure 2). Transgenic hairy roots overexpressing miR156b or miR156f were induced from *T. hemsleyanum*. The number of root branches and the total root length was significantly improved in both transgenic lines relative to the WT line. However, there were no significant differences in average root diameter (Table 2). These results suggest that the

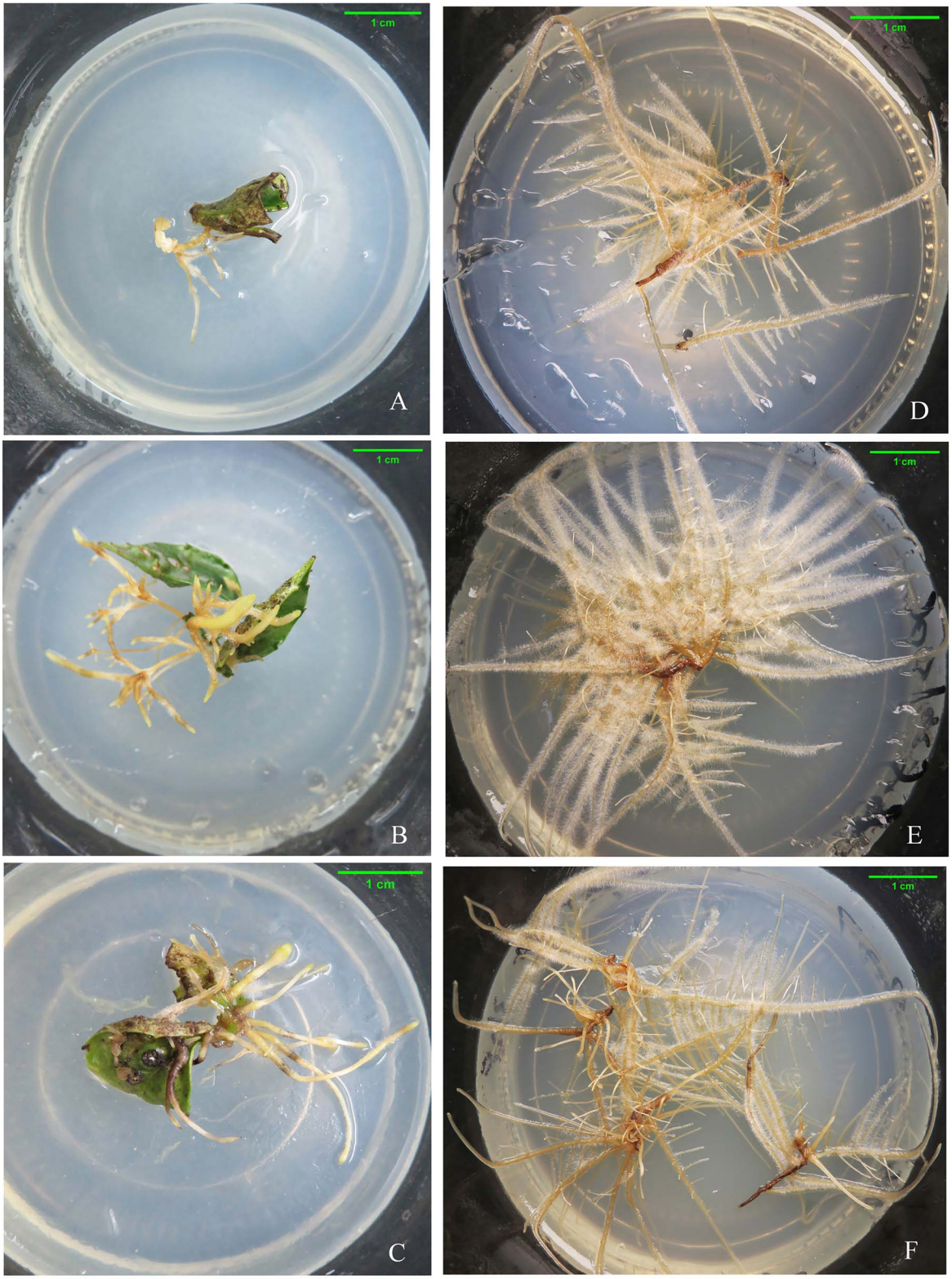

Figure 6. Transgenic hairy root induction and propagation. A, B, C: Hairy roots induced from leaves infected by WT K599, K599 with plasmid for miR156b overexpression and K599 with plasmid for miR156f overexpression, respectively; D, E, F: Hairy roots of the WT, miR156b-overexpressing and miR156f-overexpressin plants, respectively.

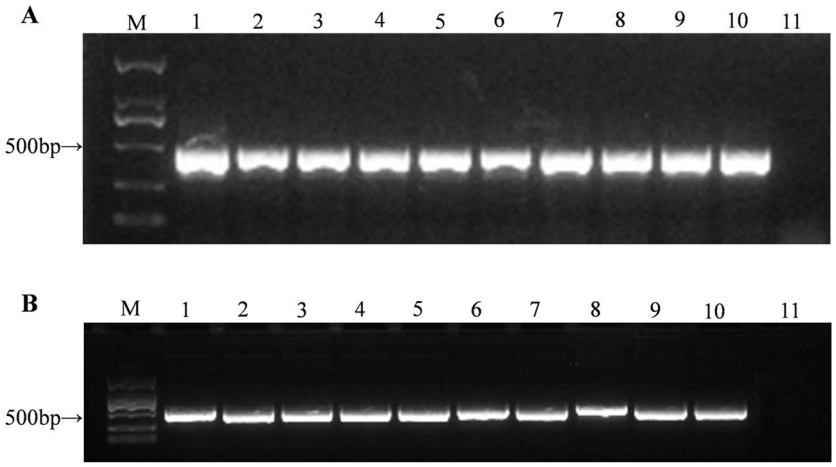

Figure 7. Identification of transgenic hairy roots by PCR. A: PCR with primers of the *rolC* gene; B: PCR with primers of the *gfp* gene; M: DL 2000 DNA molecular marker; 1–5: Hairy roots overexpressing miR156b; 6–10: Hairy roots of overexpressing miR156f; 11: Non-transformed root.

overexpression of miR156b and miR156f in *T. hemsleyanum* could promote lateral root formation.

Numerous studies have shown that plant miRNAs negatively regulate target gene expression by the direct cleavage of target gene mRNAs or the inhibition of their translation (German et al. 2008; Ji et al. 2011; Ren et al. 2014; Ma et al. 2020). Bioinformatics analysis revealed that *SPL9/10* are the target genes of miR156b and miR156b (Table 1). Meanwhile, the relative expression of *SPL9* and *SPL10* was significantly lower in the roots overexpressing miR156b and miR156f, respectively, as compared with the WT roots (Figure 9B). These results suggest that *SPL9* and *SPL10* could be the target genes of miR156b and miR156f, respectively. The fermentation broth of the endophytic strain TH15 isolated from *T. hemsleyanum* and the secondary metabolite ZEN from TH15 were found to promote root growth in *T. hemsleyanum* seedlings (Song et al. 2017; Wang et al. 2022). We therefore speculated that the ZEN secreted by strain TH15 in the roots of *T. hemsleyanum* promoted the expression of miR156b and miR156f, which in turn negatively regulated the expression of their putative target genes *SPL9* and *SPL10*, consequently promoting the growth and development of the lateral roots.

Notably, in addition to miR156b and miR156f, which were significantly up-regulated, there were other miRNAs that were up or downregulated in *T. hemsleyanum* roots treated with ZEN (Table 1). Li et al. (2010) reported that in soybean, the transgenic expression of miR482, miR1512 and miR1515 led to significant increases in nodule numbers, whereas root length, lateral root density and the number of nodule primordia were not altered in all tested miRNA lines. Zhang et al. (2019) identified pbr-miR160, pbr-miR168, pbr-miR171 and pbr-miR319, and found that the production of these miRNAs was suppressed under low levels of synthetic auxin. The targets of these miRNAs (pbARF, pbAEC, pbSCL and pbTCP4) respond to auxin signaling pathways in pear. Li et al. (2018*a*, 2018*b*) reported that the mRNA level of genes encoding the auxin response factor LaARF1 and the content of indole-3-acetic acid were significantly increased in LaMIR166a-overexpressing *Larix leptolepis*, and miR166a played a role in auxin biosynthesis and signaling during somatic embryogenesis. The overexpression of miR166f in mulberry could increase the activity of enzymes associated with drought tolerance and the accumulation of soluble proteins, reduce the content of malonaldehyde as a measure of oxidative stress and enhance drought tolerance. Li et al. (2020) found that miR166 played an important role in the interaction between auxin and abscisic acid in maize.

Moreover, ZEN was reported to influence plant growth and development through various mechanisms, such as by regulating the state and function of plant photosynthetic organs and stimulating the photochemical reaction in PSII (Kościelniak et al. 2009), protecting the photosynthetic systems of wheat and soybean seedlings against strong illumination (Kościelniak et al. 2011) and improving the drought tolerance of maize seeds (Chen et al. 1989). In ZEN-treated *T. hemsleyanum* roots, the up or downregulation of other miRNAs may be associated with physiological processes (e.g., stress resistance and photosynthesis), via which ZEN could directly or indirectly influence plant growth and development. For example, the expression of miR164a was significantly upregulated in *T. hemsleyanum* treated with ZEN, and thus it may play a regulatory role in the response to biological stress by negatively regulating the expression of NAC transcription factors. miR171a was significantly upregulated in *T. hemsleyanum* treated with ZEN, affecting the expression of the transcription factor GRAS, which may play an important role in root cell elongation and auxin signal transduction. Furthermore, miR166a-p5 was significantly upregulated in ZEN-treated *T. hemsleyanum*, and its putative target gene *MAPKKK* may be involved in the regulation of MAPK signaling.

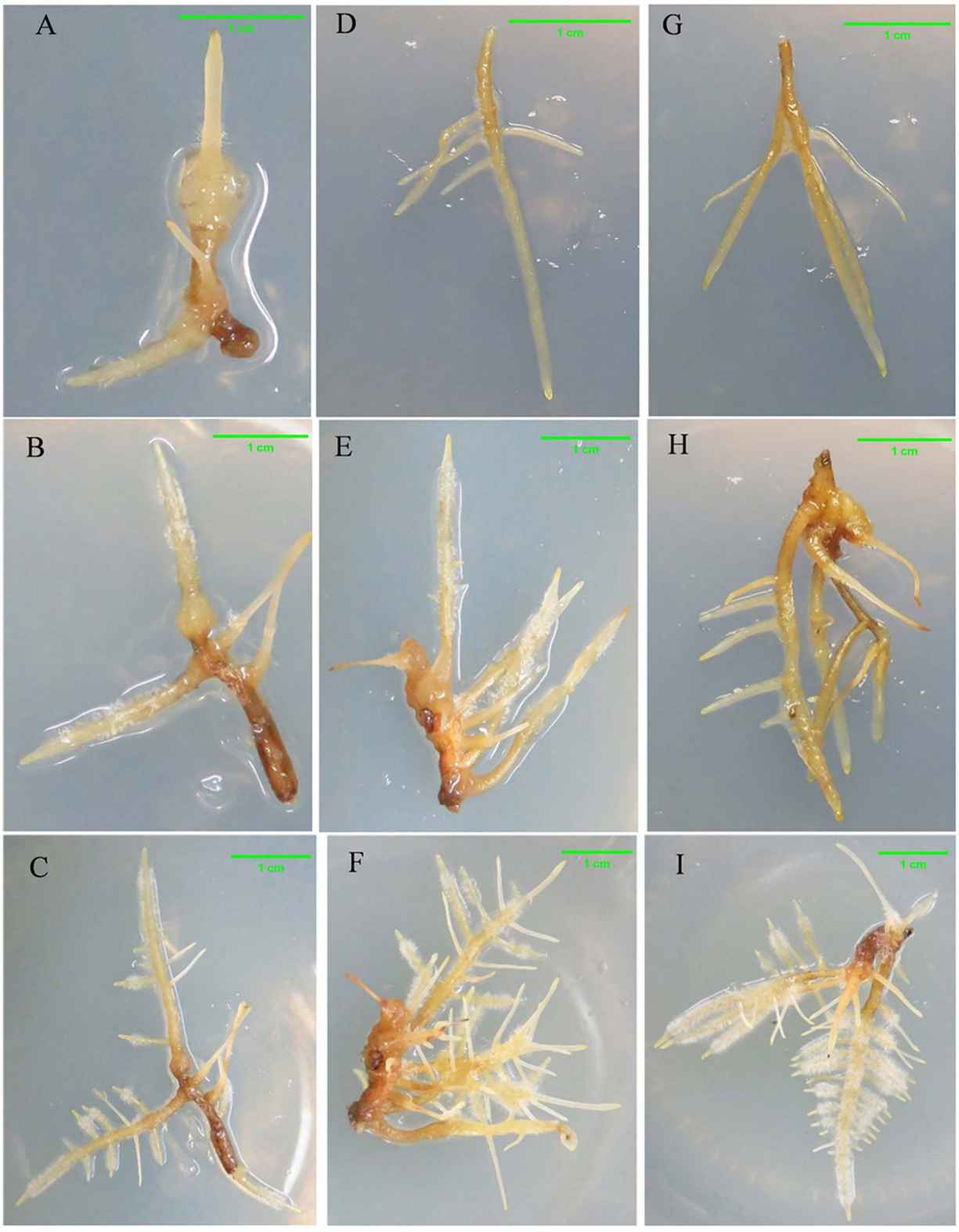

Figure 8. Growth characteristics of the hairy roots after 1 month of culture. A, B, C: WT hairy roots cultured for 10, 20 and 30 days; D, E, F: miR156b-overexpressing hairy roots cultured for 10, 20 and 30 days; G, H, I: miR156f-overexpressing hairy roots cultured for 10, 20 and 30 days.

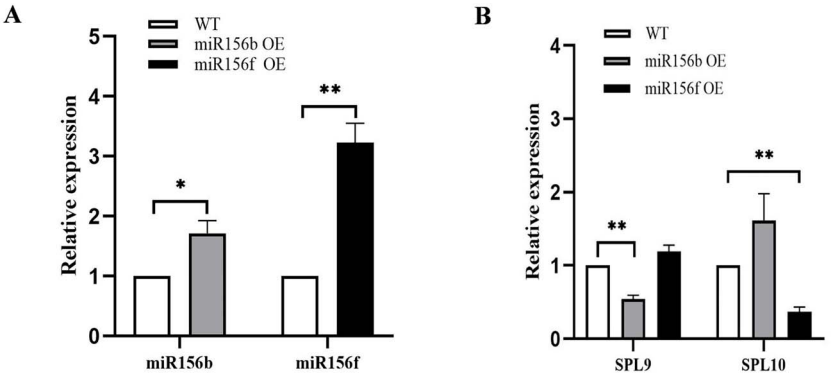

Figure 9. Relative expression levels of miR156 and predicted target genes in the transgenic hairy roots analyzed by qRT-PCR. A: Relative expression of miR156b in miR156b OE hairy roots, and miR156f in miR156f OE hairy roots; B: Relative expression of *SPL9* and *SPL10* in the miR156b OE and miR156f OE hairy roots; values are mean ± SE ($n = 3$); $^{*}P < 0.05$; $^{**}P < 0.01$, Student's *t*–test.

Conclusion

In this study, the roots of *T. hemsleyanum* seedlings treated with and without ZEN were subjected to high-throughput miRNA sequencing and *A. rhizogenes*-mediated transformation, and miRNAs exhibiting differential expression were identified. The functions of differential miR156 were validated in the transgenic hairy roots. (i) There were 70 miRNAs that were significantly differentially expressed between the seedlings treated with and without ZEN, seven of which were highly conserved. (ii) The lateral root number and total root length of the transgenic hairy roots overexpressing miR156b or miR156f were significantly improved as compared with the WT hairy roots, indicating that the overexpression of miR156b and miR156f in *T. hemsleyanum* promoted lateral root development. In *T. hemsleyanum*, the predicted target genes of miR156b and miR156f were *SPL9* and *SPL10*, respectively. It was found that the regulation of miR156b and miR156f by ZEN could modulate *T. hemsleyanum* root development through the negative regulation of their target genes *SPL9* and *SPL10*.

Supplementary data

Supplementary data for this article are available at *Tree Physiology* Online.

Acknowledgments

We would like to thank Hangzhou Lianchuan Biotechnology Company Ltd for assistance in the testing of the miRNAs.

Funding

The project was supported by grants from the National Natural Science Foundation of China (grant No. 31872181).

Conflicts of interest

The authors declare that they have no conflicts of interest.

Authors' contributions

T.X. conceived the project and designed the studies; J.L., X.H., Z.Z. and Z.C. conducted the analysis of miRNAs; J.L., J.H. and C.H. conducted the induction and propagation of the hairy roots. J.L. and X.H. conducted the verification by qRT-PCR; T.X., J.L., X.H. and J.H. wrote the manuscript.

Data and materials availability

All relevant information is included in tables, figures or supplementary data.

References

Arshad M, Feyissa BA, Amyot L, Aung B, Hannoufa A (2017) MicroRNA156 improves drought stress tolerance in alfalfa (*Medicago sativa*) by silencing *SPL13*. Plant Sci 258:122–136.

Ashburner M, Ball CA, Blake JA et al. (2000) Gene ontology: tool for the unification of biology. The gene ontology consortium. Nat Genet 25:25–29.

Aung B, Gao R, Gruber MY, Yuan ZC, Sumarah M, Hannoufa A (2017) MsmiR156 affects global gene expression and promotes root regenerative capacity and nitrogen fixation activity in alfalfa. Transgenic Res 26:541–557.

Aung B, Gruber MY, Amyot L, Omari K, Bertrand A, Hannoufa A (2015) MicroRNA156 as a promising tool for alfalfa improvement. Plant Biotechnol J 13:779–790.

Balcells I, Cirera S, Busk PK (2011) Specific and sensitive quantitative RT-PCR of miRNAs with DNA primers. BMC Biotechnol 11:70.

Bao ML, Bian HW, Zha YL, Li FY, Sun YZ, Bai B, Chen ZH, Wang JH, Zhu MY, Han N (2014) miR396a-mediated basic helix-loop-helix transcription factor *bHLH74* repression acts as a regulator for root growth in Arabidopsis seedlings. Plant Cell Physiol 55:1343–1353.

Barrera-Rojas CH, Otoni WC, Nogueira FTS (2021) Shaping the root system: the interplay between miRNA regulatory hubs and phytohormones. J Exp Bot 72:6822–6835.

Barrera-Rojas CH, Rocha GHB, Polverari L et al. (2020) miR156-targeted *SPL10* controls Arabidopsis root meristem activity and root-derived *de novo* shoot regeneration via cytokinin responses. J Exp Bot 71:934–950.

Biesaga-Kościelniak J, Marcińska I, Wedzony M, Kościelniak J (2003) Effect of zearalenone treatment on the production of wheat haploids via the maize pollination system. Plant Cell Rep 21:1035–1039.

Bosch U, Mirocha CJ (1992) Toxin production by Fusarium species from sugar beets and natural occurrence of zearalenone in beets and beet fibers. Appl Environ Microbiol 58:3233–3239.

Cai H, Yang CX, Liu S, Qi HR, Wu L, Xu LA, Xu M (2019) MiRNA-target pairs regulate adventitious rooting in *Populus*: a functional role for miR167a and its target auxin response factor 8. Tree Physiol 39:1922–1936.

Chen X, Liu H, Meng F (1989) Direct enzyme-linked immunoassay for zearalenone. Plant Physiol Commun 5:61–83 (in Chinese).

Couzigou JM, Combier JP (2016) Plant microRNAs: key regulators of root architecture and biotic interactions. New Phytol 212:22–35.

Du S, Xiang TH, Song YL, Huang LX, Sun Y, Han YX (2015) Transgenic hairy roots of *Tetrastigma hemsleyanum*: induction, propagation, genetic characteristics and medicinal components. Plant Cell Tiss Org Cult 122:373–382.

Eagles EJ, Benstead R, Macdonald S, Handy R, Hutchinson TH (2019) Impacts of the mycotoxin zearalenone on growth and photosynthetic responses in laboratory populations of freshwater macrophytes (Lemna minor) and microalgae (Pseudokirchneriella subcapitata). Ecotoxicol Environ Saf 169:225–231.

Filek M, Sieprawska A, Kościelniak J, Oklestkova J, Jurczyk B, Telk A, Biesaga-Kościelniak J, Janeczko A (2019) The role of chloroplasts in the oxidative stress that is induced by zearalenone in wheat plants–the functions of 24-epibrassinolide and selenium in the protective mechanisms. Plant Physiol Biochem 137:84–92.

Friedländer MR, Chen W, Adamidi C, Maaskola J, Einspanier R, Knespel S, Rajewsky N (2008) Discovering microRNAs from deep sequencing data using miRDeep. Nat Biotechnol 26:407–415.

Fu YF, Meng FJ (1994) Zearalenone in growth and development of winter wheat. Acta Agron Sin 20:271–276 (in Chinese).

Gaddam SR, Bhatia C, Sharma A, Badola PK, Saxena G, Trivedi PK (2021) miR775 integrates light, sucrose and auxin associated pathways to regulate root growth in *Arabidopsis thaliana*. Plant Sci 313:111073.

Gao R, Wang Y, Gruber MY, Hannoufa A (2018) miR156/SPL10 modulates lateral root development, branching and leaf morphology in Arabidopsis by silencing *AGAMOUS-LIKE 79*. Front Plant Sci 8: 2226.

Gautier C, Pinson-Gadais L, Richard-Forget F (2020) Fusarium mycotoxins enniatins: an updated review of their occurrence, the producing Fusarium species, and the abiotic determinants of their accumulation in crop harvests. J Agric Food Chem 68:4788–4798.

German MA, Pillay M, Jeong DH et al. (2008) Global identification of microRNA-target RNA pairs by parallel analysis of RNA ends. Nat Biotechnol 26:941–946.

Huang XP, Zeng ZH, Chen ZH, Yang YJ, Pang JL, Qian YS, Xiang TH (2022) Whole-genome sequence resource of *Fusarium oxysporum* strain TH15, a plant growth promoting endophytic fungus isolated from *Tetrastigma hemsleyanu*. PhytoFrontiers 2on line first. https://doi.org/10.1094/PHYTOFR-12-21-0086-A.

Jerome Jeyakumar JM, Ali A, Wang WM, Thiruvengadam M (2020) Characterizing the role of the miR156-SPL network in plant development and stress response. Plants (Basel) 9:1206.

Ji LJ, Liu XG, Yan J et al. (2011) *ARGONAUTE10* and *ARGONAUTE1* regulate the termination of floral stem cells through two microRNAs in Arabidopsis. PLoS Genet 7:e1001358.

Kanehisa M, Goto S (2000) KEGG: Kyoto encyclopedia of genes and genomes. Nucleic Acids Res 28:27–30.

Kościelniak J, Biesaga-Kościelniak J, Janeczko A, Filek W, Kalaji HM (2009) Can the *Giberella zeae* toxin zearalenone affect the photosynthetic productivity and increase yield formation in spring wheat and soybean plants. Photosynthetica 47:586–594.

Kościelniak J, Ostrowska A, Biesaga-Kościelniak J, Filek W, Janeczko A, Kalaji HM, Stalmach K (2011) The effect of zearalenone on PSII photochemical activity and growth in wheat and soybean under salt (NaCl) stress. Acta Physiol Plant 33:2329–2338.

Li H, Deng Y, Wu T, Subramanian S, Yu O (2010) Misexpression of miR482, miR1512, and miR1515 increases soybean nodulation. Plant Physiol 153:1759–1770.

Li HX, Meng FJ (1989) Isolation and identification of zearalenone from *Apium graveoleus*. Plant Physiol J 15:211–215 (in Chinese).

Li JL, Zhu TX, Zhang C, Li BR, Deng ZP, Li YS, Meng FJ (1980) Studies on zearalenone. J China Agric Univ 1:13–28 (in Chinese).

Li N, Yang TX, Guo ZY et al. (2020) Maize microRNA166 inactivation confers plant development and abiotic stress resistance. Int J Mol Sci 21:9506.

Li RX, Fan T, Wang TC et al. (2018*a*) Characterization and functional analysis of miR166f in drought stress tolerance in mulberry (*Morus multicaulis*). Mol Breed 38:132.

Li X, Shahid MQ, Wu JW, Wang L, Liu XD, Lu YG (2016) Comparative small RNA analysis of pollen development in autotetraploid and diploid rice. Int J Mol Sci 17:499.

Li ZX, Fan YR, Dang SF, Li WF, Qi LW, Han SY (2018*b*) LaMIR166a-mediated auxin biosynthesis and signaling affect somatic embryogenesis in *Larix leptolepis*. Mol Genet Genomics 293: 1355–1363.

Luo M, Gao Z, Li H, Li Q, Zhang C, Xu W, Song S, Ma C, Wang S (2018) Selection of reference genes for miRNA qRT-PCR under abiotic stress in grapevine. Sci Rep 8:4444–4454.

Ma LJ, Geiser DM, Proctor RH, Rooney AP, O'Donnell K, Trail F, Gardiner DM, Manners JM, Kazan K (2013) Fusarium pathogenomics. Annu Rev Microbiol 67:399–416.

Ma X, Ibrahim F, Kim EJ, Shaver S, Becker J, Razvi F, Cerny RL, Cerutti H (2020) An ortholog of the vasa intronic gene is required for small RNA-mediated translation repression in *Chlamydomonas reinhardtii*. Proc Natl Acad Sci U S A 117:761–770.

Mally A, Solfrizzo M, Degen GH (2016) Biomonitoring of the mycotoxin zearalenone: current state-of-the art and application to human exposure assessment. Arch Toxicol 90:1281–1292.

Meng F-J, Que Y-M, Han Y-Z, Li H-X, Wang Z-C (1989) Isolation of zearalenone from shoot apices of overwintering winter wheat. Sci China B 32:1100–1105.

Munkvold GP (2017) Fusarium species and their associated mycotoxins. Methods Mol Biol 1542:51–106.

Pfaffl MW (2001) A new mathematical model for relative quantification in real-time RT-PCR. Nucleic Acids Res 29:e45.

Rai A, Das M, Tripathi A (2020) Occurrence and toxicity of a fusarium mycotoxin, zearalenone. Crit Rev Food Sci Nutr 60:2710–2729.

Ren GD, Xie M, Zhang SX, Vinovskis C, Chen XM, Yu B (2014) Methylation protects microRNAs from an AGO1-associated activity that uridylates 5' RNA fragments generated by AGO1 cleavage. Proc Natl Acad Sci U S A 111:6365–6370.

Song YL, Wu P, Li YF, Tong XX, Zheng YF, Chen ZH, Wang LL, Xiang TH (2017) Effect of endophytic fungi on the host plant growth, expression of expansin gene and flavonoid content in *Tetrastigma hemsleyanum* Diels & Gilg *ex* Diels. Plant Soil 417:393–402.

Sun Z, Su C, Yun J et al. (2019) Genetic improvement of the shoot architecture and yield in soya bean plants via the manipulation of *GmmiR156b*. Plant Biotechnol J 17:50–62.

Tang C, Han RP, Zhou ZK, Yang YY, Zhu MK, Xu T, Wang AM, Li ZY, Dong TT (2020) Identification of candidate miRNAs related in storage root development of sweet potato by high throughput sequencing. J Plant Physiol 251:153224.

Tong X, Li Y, Xiang T, Chen Z, Wang L, Zhang C, Feng M, Wu L (2018) The complete genome sequence of cucumopine-type *Agrobacterium rhizogenes* strain K599 (NCPPB2659), a nature's genetic engineer inducing hairy roots. Int J Agric Biol 20:1167–1174.

Wang LZ, Huang XP, Li JS, Huang JX, Bao SY, He CJ, Zhang MM, Xiang TH (2022) Metabolites of zearalenone and phytohormones secreted by endophytic fungus strain TH15 regulating the root development in *Tetrastigma hemsleyanum*. Plant Cell Tiss Org Cult 150:683–694.

Weigt D, Niemann J, Siatkowski I, Zyprych-Walczak J, Olejnik P, Kurasiak-Popowska D (2019) Effect of zearalenone and hormone regulators on microspore embryogenesis in anther culture of wheat. Plants (Basel) 8:487.

Williamson V, Kim A, Xie B, McMichael GO, Gao Y, Vladimirov V (2013) Detecting miRNAs in deep-sequencing data: a software performance comparison and evaluation. Brief Bioinform 14:36–45.

Wu CH, Apweiler R, Bairoch A et al. (2006) The universal protein resource (UniProt): an expanding universe of protein information. Nucleic Acids Res 34:D187–D191.

Xiang TH, Li JS, Bao SY, Xu ZX, Wang LZ, Long FZ, He CJ (2021) Digital RNA-seq transcriptome plus tissue anatomy analyses reveal the developmental mechanism of the calabash-shaped root in *Tetrastigma hemsleyanum*. Tree Physiol 41:1729–1748.

Xie K, Shen J, Hou X, Yao J, Li X, Xiao J, Xiong L (2012) Gradual increase of miR156 regulates temporal expression changes of numerous genes during leaf development in rice. Plant Physiol 158:1382–1394.

Xu M, Hu T, Zhao J, Park MY, Earley KW, Wu G, Yang L, Poethig RS (2016) Developmental functions of miR156-regulated SQUAMOSA PROMOTER BINDING PROTEIN-LIKE (*SPL*) genes in *Arabidopsis thaliana*. PLoS Genet 12:e1006263.

Xu X, Li X, Hu X, Wu T, Wang Y, Xu X, Zhang X, Han Z (2017) High miR156 expression is required for auxin-induced adventitious root formation via *MxSPL26* independent of *PINs* and *ARFs* in *Malus xiaojinensis*. Front Plant Sci 8:1059.

Yang K, Deng Y, Zhang C, Elasri M (2006) Identification of new members of hydrophobin family using primary structure analysis. BMC Bioinformatics Suppl 4:S16.

Yao K, Zhang F, Meng F (1991) Biological effects of zearalenone in tissue culture (bulletin). Plant Physiol Commun 27:29–31 (in Chinese).

Yao KL, Meng FJ (1991) A novel plant growth regulator: zearalenone. Beijing Agric Sci 6:6–8 (in Chinese).

Yu G, Wang LG, Han Y, He QY (2012) clusterProfiler: an R package for comparing biological themes among gene clusters. OMICS 16:284–287.

Yu N, Niu QW, Ng KH, Chua NH (2015) The role of miR156/SPLs modules in *Arabidopsis* lateral root development. Plant J 83: 673–685.

Yuan L, Wu H, Peng X, Qiu D, Tao Z, Qiu W (2020) Reference genes selection and system establishment for RT-qPCR of *T. hemsleyanum* in root development stages. Mol Plant Breed 18:6785–6792 (in Chinese).

Yun J, Sun Z, Jiang Q et al. (2022) The miR156b-GmSPL9d module modulates nodulation by targeting multiple core nodulation genes in soybean. New Phytol 233:1881–1899.

Zhang L, Ding H, Jiang H, Wang H, Chen K, Duan J, Feng S, Wu G (2020) Regulation of cadmium tolerance and accumulation by miR156 in Arabidopsis. Chemosphere 242:125168.

Zhang Q, Zhang Y, Wang S, Hao L, Wang S, Xu C, Jiang F, Li T (2019) Characterization of genome-wide microRNAs and their roles in development and biotic stress in pear. Planta 249:693–707.

Zhao DG, Meng FJ (1999) Involvement of zearalenone in short day vernalization in winter wheat. Plant Physiol J 25:66–72 (in Chinese).

Zhou J, Lu Y, Shi WG, Deng SR, Luo ZB (2020) Physiological characteristics and RNA sequencing in two root zones with contrasting nitrate assimilation of *Populus* × *canescens*. Tree Physiol 40: 1392–1404.